A PROBABILISTIC HIGH CYCLE FATIGUE MODEL APPLIED TO CAST Al-Si ALLOYS

I. Koutiri[a], D. Bellett[a], F. Morel[a,] and L. Augustins[b]

[a] LAMPA, Arts et Métiers ParisTech, Angers, France
[b] PSA Peugeot Citroën, Route de Gisy, 78943 Vélizy-Villacoublay Cedex, Case courrier VV1415, France

Abstract In this work, the high cycle fatigue behavior of cast hypo-eutectic Al-Si alloys is investigated. It is observed that two different coexisting fatigue initiation mechanisms can occur in these materials depending on the presence of different microstructural heterogeneities (i.e. micro-shrinkage pores, Si particles, Fe-rich inter-metallics, DAS of the Al-matrix, etc).
Firstly, an experimental study is presented, highlighting the coexistence of these two fatigue damage mechanisms and their dependence on the presence of different micro-structural heterogeneities. A probabilistic high cycle fatigue model, which has the capacity to describe these two mechanisms, is then presented. The model contains the same principal ingredients as the one developed by [Pessard et al 2011]. It uses a probabilistic framework to link the two different fatigue damage mechanisms, and can take into account the mean stress and the effect of a biaxial stress state.

1 INTRODUCTION

Due to their favourable combination of physical and mechanical properties, cast aluminium alloys have received much use in the automobile industry. One example is the casting of aluminium cylinder heads for automobile engines. These components have a very complicated geometry due to the admission, exhaust and cooling passages and the valve control system, but are essential to the correct operation of the engine. In order to ensure that these components conform to their required specifications, numerical modelling techniques are employed [Comte el al 2005]. The results from these simulations show that certain zones of these components are subjected to complex multiaxial cyclic stress-stain states, including high mean stress. Hence, the high cycle fatigue design of these components requires the use of fatigue criteria which are adapted to the material and the loading conditions. The development of an appropriate criterion, for this application, is the object of this work. However, prior to discussing the criterion, fatigue damage mechanisms for different loading modes are discussed. In the literature there exists a considerable amount of uniaxial fatigue data (either in rotating bending, plane bending or uniaxial tension-compression). On the other hand, very little data is available concerning bi-axial tensile loading modes and torsion. The principal objectives of this article are to investigate these two loading modes, to highlight the co-existence of two different fatigue damage mechanisms observed in the material and to propose a fatigue model adapted to the material and the loading conditions.

2 MATERIAL: AlSi7Cu05Mg03-T7 (A356-T7)

Fatigue specimens were made from material taken from cylinder heads, manufactured by PSA for use in diesel automobile engines. The cylinder heads were gravity sand cast. During the casting process titanium and boron are added to the liquid metal in order to refine the size of the alpha-phase dendrites. Strontium is added to modify the shape of the silicon eutectic particles. The cast components are subsequently quenched and age hardened. The resulting mechanical properties of the material are listed in Table 1.

0.2% Yield stress, Σ_Y	**Ultimate tensile strength, Σ_{uts}**	**Percent elongation at rupture, A%**
250 - 260 MPa	318 - 330 MPa	5.0 - 5.7 %

Table 1 - Mechanical properties of AlSi7Cu05Mg03-T7

Figure 1 shows the material microstructure created as a result of the process described above. The material is composed of alpha-phase dendrites with an average Dendrite Arm Spacing (DAS) of approximately 80 µm. The eutectic silicon particles are fine and spherical. The dark feature in Figure 1 is a casting defects (i.e. a micro-shrinkage pore) caused by the shrinkage of the molten liquid during solidification. In a complicated gravity cast component like a cylinder head it is impossible to completely eliminate this type of defect. The presence of intermetallic precipitates can also be distinguished.

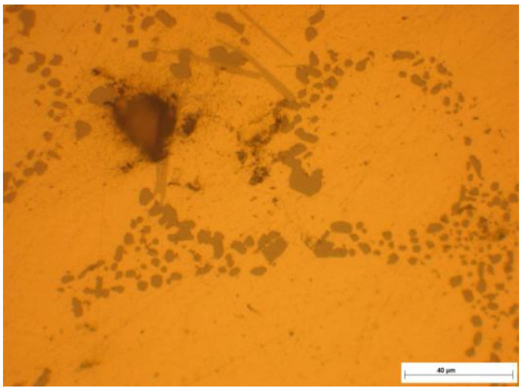

Figure 1. Microstructure of AlSi7Cu05Mg03

3 EXPERIMENTAL CONDITIONS – FATIGUE TESTS

All of the fatigue tests presented below were conducted at ambient temperature and pressure.

3.1 Plane bending fatigue tests

A series of uniaxial plane bending fatigue tests were undertaken, with the aim of identifying the effect of the mean stress. Five different load ratios have been investigated:

- R = -1 (Zero mean stress, $\Sigma_\mathrm{m} = 0$ MPa).
- R = 0.1.
- R = 0.62 (with the maximum stress slightly less than the yield stress, $\Sigma_{max} \approx \Sigma_Y$).
- R = 0.88 (with the mean stress equal to the yield stress, $\Sigma_m = \Sigma_Y$).
- R = 0.92 (with the maximum stress slightly less than the ultimate tensile strength, $\Sigma_{max} \approx \Sigma_{uts}$).

For each load ratio, the fatigue strength at 2×10^6 cycles was determined via the staircase method with a minimum of 10 specimens. All tests were done using a RUMUL Cracktronic electo-magnetic resonance fatigue testing machine. The test frequency was approximately 80 Hz. Tests were stopped when a drop in frequency of 0.1Hz was detected. This corresponds to the presence of cracks of approximately 3mm long.

3.2 Torsional fatigue tests

Torsional fatigue tests, with zero mean stress (R=-1), were also done. The RUMUL Cracktronic machine was used with the same testing conditions as described above.

3.3 Biaxial tensile fatigue tests

Concerning the biaxial fatigue tests, it was not possible to make hollow specimens for tension/internal pressure type tests as the volume of material available to fabricate the specimens was too small. Therefore, an axisymmetrical bending testing apparatus was developed to undertake these tests (see Figure 2). This test setup forms the object of a French national patent submitted in May 2011 [Duparque et al 2011]. Disk shaped specimens with a reduction in thickness on the compressive side of the specimen are tested (see Figure 2(b)). The tests were conducted using a servo-hydraulic INSTRON 8802 fatigue testing machine. An equibiaxial stress state is obtained at the centre of the specimen. In order to verify the local strain state and to detect fatigue crack initiation, a uniaxial strain gauge was glued at the centre of the compressive side of each specimen in the flat part of the reduced thickness zone (see Figure 2(b)). The minimum value of strain per cycle was recorded. The appearance of a fatigue crack on the tensile side of the specimen results in a change in the measured strain field.

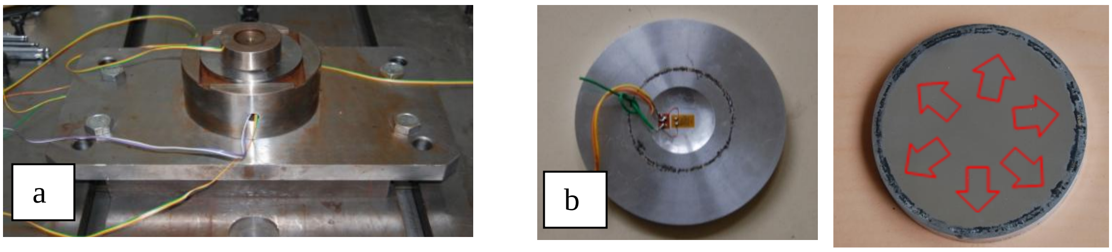

Figure 2. (a) An axisymmetrical bending testing apparatus for equibiaxial fatigue testing (b) Disk shaped test specimen (strain gauge shown on the compressive side)

Note that only positive load ratios can be tested using this setup, and that the equibiaxial stress state is proportional and in-phase. The equibiaxial fatigue limit at $2x10^6$ cycles has been determined for a load ratio of R=0.1 using the staircase method (with 9 specimens). The tests were conducted at a frequency of 20Hz.

4 FATIGUE BEHAVIOUR

4.1 The mean stress effect: AlSi7Cu05Mg03-T7

Figure 3 shows the totality of the uniaxial fatigue results, discussed above, presented in the form of a Wöhler diagram, for the different load ratios tested. Note that the results obtained by [Bellett et al 2005] for the same material, tested in uniaxial tension and for two different load ratios, are also shown.

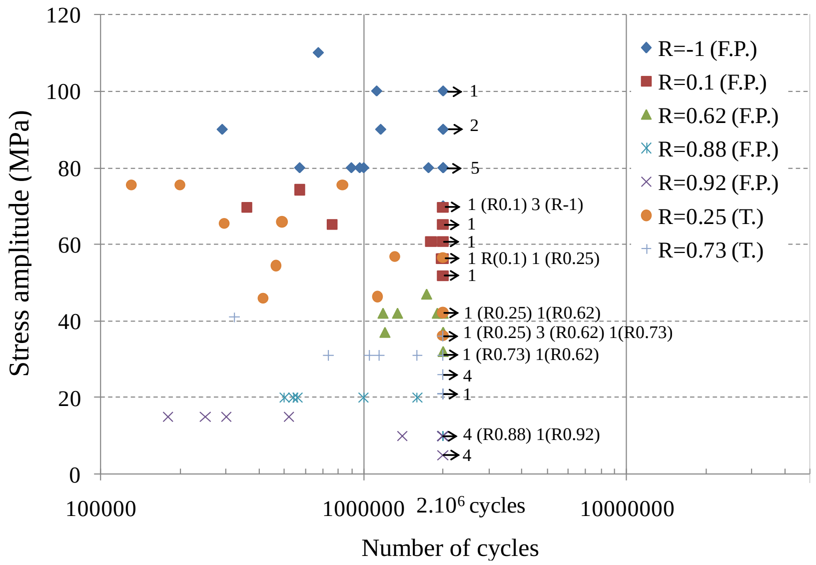

Figure 3. Wöhler diagram for AlSi7Cu05Mg03 (F.P. = Plane Bending and T. = Tension [Bellett et al 2005])

It is important to note that, even for the high load ratios (R = 0.88 and 0.92) a fatigue limit at $2x10^6$ cycles exists. These load ratios correspond to high mean stress and small stress amplitude, where the maximum stress is close to the ultimate tensile strength of the material.

Table I. Uniaxial fatigue results

Plane Bending			
Σ_{moy} (MPa)	*Σ_{amp} (MPa)*	*Load Ratio*	*Standard deviation (MPa)*
0	82.5	-1	27.8
77	63.1	0.1	32.8
195.5	44.5	0.62	7
251	15	0.88	5.3
283.5	11.5	0.92	5.3
Uniaxial Tension [Bellett et al 2005]			
82.5	51	0.25	11.1
172	26	0.73	5.1

Table I summarises the uniaxial results in terms of the fatigue limits at $2x10^6$ cycles for 50% probability of failure. Concerning the dispersion, which has be quantified via the staircase method (even if the number of specimens are on the low side), the observed tendency is that the scatter decreases with increasing mean stress. More precisely, for the low load ratios (R=-1 and 0.1) the dispersion is very high, however it is dramatically reduced at the high load ratios. This seems to indicate that the fatigue damage mechanism can change as a function of the load ratio.

4.2 The effect of an equibiaxial stress state

For the cast aluminium alloy in question, Figure 4 shows the comparison between the uniaxial and equibiaxial fatigue test results for a load ratio of R=0.1.

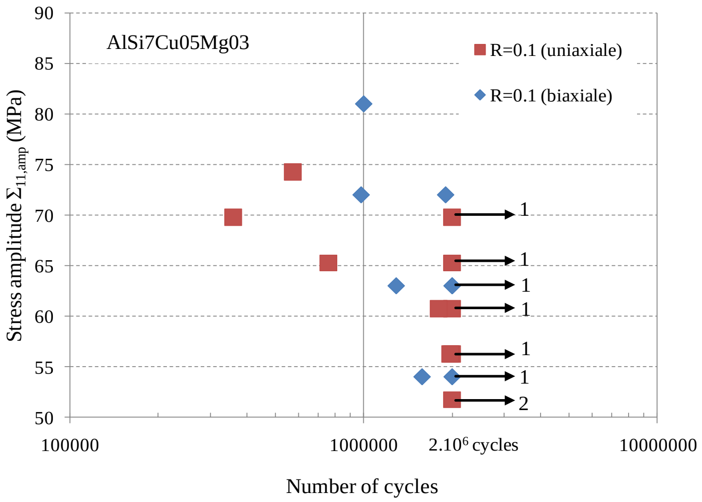

Figure 4. Wohler diagram for AlSi7Cu05Mg03 (R=0.1, plane bending: uniaxial stress state and R=0.1, axisymmetrical bending: equibiaxial stress state)

This diagram highlights the fact that the dispersion for both loading types is basically the same, and more surprisingly it shows that there is very little difference between the average fatigue limits at $2x10^6$ cycles. This implies that an equibiaxial loading condition does not result in greater fatigue damage than the uniaxial case (at least for this material).

5 FATIGUE DAMAGE MECHANISMS

5.1 Uniaxial loads

Much research has been reported in the scientific literature concerning the fatigue initiation mechanisms in cast aluminium alloys, which is generally related to uniaxial loads at low R-ratios (i.e. R=-1 or 0.1). This body of work makes it apparent that due to the different microstructural heterogeneities present in the material, fatigue crack initiation sites can be varied. However, when micro-shrinkage pores are present they play the fundamental role in controlling fatigue behaviour. Their size, position, distribution, etc, have a large impact on the fatigue resistance of the material. When specific treatments, such as HIP (Hot Isostatic Pressing), are used to obtain a microstructure which is practically void of micro-shrinkage pores, crack initiation occurs at other microstructural heterogeneities, such as oxide inclusions, silicon eutectic particles or intermetallic precipitates. This relationship between crack initiation and the degree of porosity present in the microstructure has been largely documented in the literature [Inguanti 1985, Murali et al 1997, Powell 1994, Skallerud 1993].

In this work, numerous fatigue damage observations have been undertaken using specimens made from material extracted from cylinder heads cast by PSA. Both surface observations (using an optical microscope during cycling) and observations of the fatigue failure surfaces (using an SEM) have been done. These observations show that for plane bending and uniaxial tensile loads with an R-ratio of R=-1, initiation of the fatigue crack resulting in final failure of the specimens almost always occurs at a micro-shrinkage pore (see Figure 5).

It is very important to note however, that in the same specimens, micro-cracks are observed to initiate at Silicon rich particles in the eutectic zones or at intermetallic precipitates (see Figure 6). For the material and loading conditions in question, this type of damage is not generally responsible for the final failure of the specimen, but it does exist.

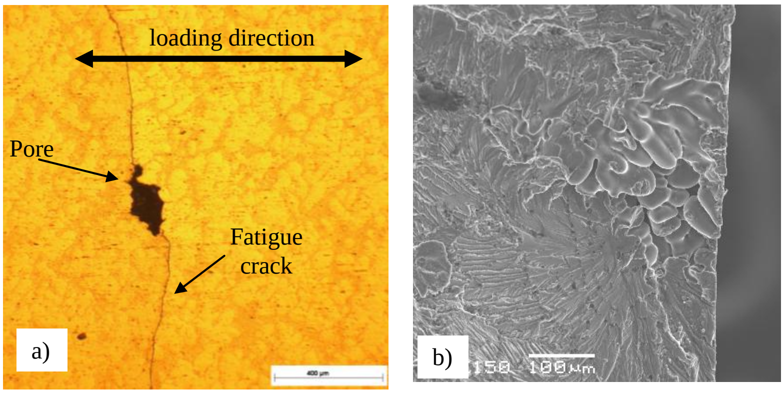

Figure 5. Fatigue crack initiation from a micro-shrinkage pore in AlSi7Cu05Mg03, loaded uniaxially with an R-ratio of R=-1 a) Surface observation b) SEM image of a failure surface

It is therefore concluded that fatigue damage in this material is controlled by two different fatigue crack initiation mechanisms: One mechanism is associated with relatively large micro-shrinkage pores and the other is controlled by much smaller microstructural heterogeneities or the material matrix.

It is proposed that the first mechanism is basically a problem of crack propagation, or more precisely, of non-propagation. That is, fatigue cracks initiate very quickly at micro-shrinkage pores and the fatigue strength is then controlled by the ability of the microstructure to prevent the propagation of these cracks (see Figure 6b)). In the following section this mechanism will be described via a fracture mechanics approach.

The second mechanism, in which the fatigue damage occurs at a smaller scale, it is assumed that crack initiation is controlled by localised plasticity, related to the micro-structural heterogeneities in question, or simply the material matrix. A multi-scale fatigue criterion based on the concept of elastic shakedown is used in the following section to describe this fatigue damage mechanism.

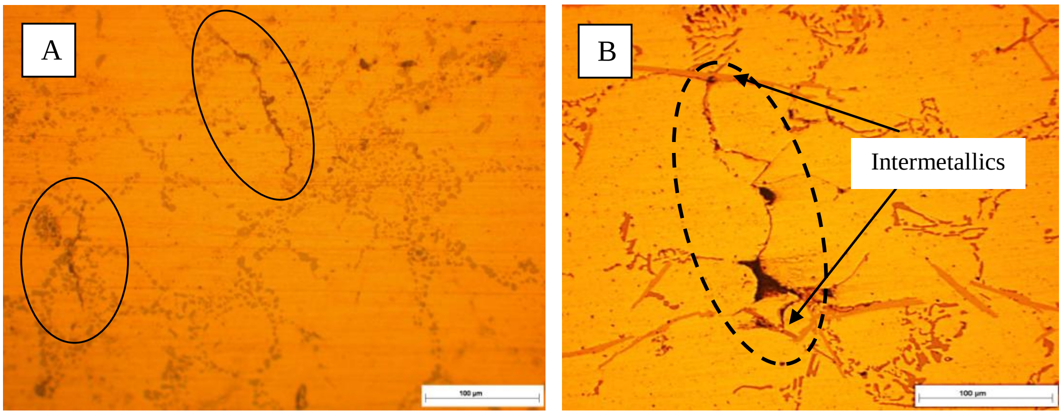

Figure 6. a) Fatigue crack initiation at Si-particles in the eutectic zones b) Initiation from a micro-shrinkage pore for which the crack propagation has been stopped by the presence of microstructural barriers (intermetallic precipitates) in AlSi7Cu05Mg03 for uniaxial loads with an R-ratio of R=-1

6 THE PROPOSED MODEL

There exist two broad philosophical approaches to high cycle metal fatigue problems. These are:

a) The safe life approach – In which a component or structure is designed so that it never fails in fatigue. The prediction of crack initiation is the key to this methodology, which is often used in conjunction with multi-scale fatigue models based on the concepts of elastic shakedown.
b) The damage tolerance approach – In which a component or structure is assumed to contain fatigue damage, or cracks, and is subsequently designed so that the damage never reaches a critical state leading to failure. This type of philosophy is very often used in conjunction with fracture mechanics approaches.

The major advantage of the model proposed in this work is that both of these approaches are used. Specifically a fracture mechanics approach is used to model the fatigue damage mechanism associated with micro-shrinkage pores and a multi-scale, multiaxial fatigue model based on the concepts of elastic shakedown is used to model the mechanism associated with failure in the material matrix. A weakest link probabilistic concept is subsequently used to combine the two models, which results naturally in a probabilistic Kitagawa type diagram. This approach uses the basic ingredients of the model proposed by Pessard and Morel [Pessard et al 2009] for the prediction of anisotropic fatigue behaviour of forged steels.

6.1 Modeling the fatigue damage occurring in the material matrix (without the presence of micro-shrinkage pores)

As discussed above, experimental observations have highlighted the presence of two co-existing fatigue damage mechanisms occurring in the AlSi7Cu05Mg03 material. The purpose of this section is to present the model used to describe the mechanism associated with the apparition of fatigue cracks in the material matrix, without the presence of micro-shrinkage pores.

In order to estimate the probability of crack initiation, P_{F1}, due to the apparition of meso-plasticity in the material matrix, the [Huyen and Morel 2008] criterion is used. This approach is based on the hypotheses of elastic shakedown at the mesoscopic scale and the weakest link theory applied to all material planes of a Representative Elementary Volume. The random character of the fatigue resistance is introduced via a Weibull distribution. The essential ingredients of this criterion are as follows.
The probability of fatigue failure can be expressed as:

$$P_{F1} = 1 - exp\left[-\frac{1}{V_{01}}\int_V \frac{{X_a}^{m_1} I_{m1}}{{T_{01}}^{m_1}} dV\right] \qquad (1)$$

Where $X_a = \max_{\theta,\phi,\psi}\{\chi_a(\theta,\phi,\psi)\}$ and $\chi_a(\theta,\phi,\psi) = T_a(\theta,\phi,\psi) + \alpha\Sigma_{n,a}(\theta,\phi)$

$T_a(\theta,\phi,\psi)$ is the shear stress amplitude in a direction defined by three angles (θ,ϕ,ψ),
$\Sigma_{n,a}(\theta,\phi)$ is the amplitude of the normal stress acting on the material plane,
m_1 is the Weibull exponent related to the scatter associated with the fatigue initiation mechanism
To simplify the notation the parameter I_{m1} is introduced and is equal to:

$$I_{m1} = \int_{\phi=0}^{2\pi}\int_{\theta=0}^{\pi}\int_{\psi=0}^{2\pi}\left(\frac{\chi_a(\theta,\phi,\psi)}{\left(1-\gamma\Sigma_{n,m}(\theta,\phi)\right)X_a}\right)^{m_1} sin\theta d\theta d\phi d\varphi \qquad (2)$$

$\Sigma_{n,m}(\theta,\phi)$ is the mean value of the normal stress acting on the material plane,
The tripple integration in equation (2) is used to take into account the crack initiation potential on each possible slip system within an elementary volume.

T_{o1} is the scale parameter of the Weibull distribution,

α and γ are material parameter used to take into account the effect of the normal stress.

It has been shown that this model results in good high cycle fatigue predictions for multiaxial loading conditions and in particular tension-torsion loads and biaxial loads [Koutiri 2011]. Out-of-phase and variable frequency loading conditions have also been successfully modeled using this criterion [Huyen 2008].

6.2 Modelling the fatigue damage due to micro-shrinkage pores

The probability that a crack will propagate from a micro-shrinkage pore, P_{F2} is taken into account using concepts from Linear Elastic Fracture Mechanics. The micro-shrinkage pores are assumed to be preexisting cracks for which mode I propagation is dominate. The range of the stress intensity factor ΔK can be estimated as a function of the applied stress range, a correction factor for the shape of the crack and the size of the crack. The no-propagation condition is defined by comparing the stress intensity factor ΔK to the crack propagation threshold of the material, ΔK_{th}. It is therefore assumed that failure occurs if:

$$\Delta K \quad > \Delta K_{th} \qquad (3)$$

The random nature of the crack propagation threshold is introduced using a Weibull distribution:

$$f_{02}(\Delta K_{th}) = \frac{m_2}{\Delta K_{th02}}\left(\frac{\Delta K_{th}}{\Delta K_{th02}}\right)^{m_2-1} exp\left[-\left(\frac{\Delta K_{th}}{\Delta K_{th02}}\right)^{m_2}\right] \qquad (4)$$

Where m_2 is the Weibull exponent controlling the dispersion and ΔK_{th02} is the scale parameter associated with the damage mechanism. The size of the micro-shrinkage defects have a definite influence on the fatigue resistance however they are not the only micro-structural heterogeneity which effect crack propagation (or non-propagation). The Weibull distribution shown in equation 5 takes into account the effect of the shrinkage pore size distribution, and the effect of the microstructure surrounding the pore, which can be more or less favourable to crack propagation (i.e. the presence of Si-particles or intermetallic precipitates or the crystallographic orientation of the aluminium rich α phase).

As per the previous approach, all cracks which are potentially active are taken into account via the calculation of $\Delta K(\theta, \varphi)$ on all possible material planes defined by the angles (θ, φ). In order to estimate the possibility of crack propagation, the weakest link hypothesis is applied to all plane of a reference volume V_0 . The probability of crack propagations is thus given as:

$$P_{F02} = P\big(\Delta K_{th} < \Delta K(\theta,\varphi)\big) = 1 - exp\left[-\frac{1}{D_{02}}\int_{\varphi=0}^{2\pi}\int_{\theta=0}^{\pi}\left(\frac{\Delta K_{th}(\theta,\varphi)}{\Delta K_{th02}}\right)^{m_2} sin\theta d\theta d\varphi\right] \qquad (5)$$

The probability of rupture, for the total volume of loaded material, can be obtained by apply the weakest link hypothesis a second time. So that:

$$P_{F2} = 1 - exp\left[-\frac{1}{V_{02}}\int_V \left\{\int_{\varphi=0}^{2\pi}\int_{\theta=0}^{\pi}\left(\frac{\Delta K(\theta,\varphi)}{\Delta K_{th02}}\right)^{m_2} sin\theta d\theta d\varphi\right\} dV\right] \qquad (6)$$

Where the stress intensity factor associated with plane (θ, φ) can be written as a function of the stress normal to the plane $\Delta\sigma(\theta, \varphi)$ and the defect size, a:

$$\Delta K(\theta,\varphi) = \Delta\sigma(\theta,\varphi)\beta\sqrt{\pi a} \qquad (7)$$

The mean stress effect on ΔK_{th} is generally associated with the concept of crack closure. The evolution of the threshold, as a function of the load ratio R, in introduced via following original proposal, which is seen to be appropriate for the cast aluminum material in question.

$$\frac{\Delta K_{th}}{\Delta K_{th0}} = f(R) = \frac{(1-R)}{(1-\kappa R)} \qquad (8)$$

Where ΔK_{th0} is crack propagation threshold for an R-ratio of R=0. The probability of rupture of the complete structure is therefore given by:

$$P_{F2} = 1 - exp\left[-\frac{1}{V_{02}}\int_V \left\{\int_{\varphi=0}^{2\pi}\int_{\theta=0}^{\pi}\left(\frac{\Delta\sigma_a(\theta,\varphi)\beta\sqrt{\pi a}}{\Delta K_{th02}}\right)^{m_2} sin\theta d\theta d\varphi\right\} dV\right] \qquad (9)$$

It is possible to simplify the expression for $P_{F2}$by introducting the factor J_{m2} which is defined as:

$$J_{m2} = \int_{\varphi=0}^{2\pi}\int_{\theta=0}^{\pi}\left(\frac{\sigma_{n,a}(\theta,\varphi)}{\Sigma_{n,a}}\right)^{m_2} sin\theta d\theta d\varphi \qquad (10)$$

Where $\Sigma_{n,a} = \max_{\theta,\varphi}\{\sigma_a(\theta,\varphi)\}$

The final expression becomes: $P_{F2} = 1 - exp\left[-\frac{1}{V_{02}}\int_V \frac{{\Sigma_{n,a}}^{m_2} J_{m2}}{\Sigma_{02}(R)^{m_2}} dV\right]$

where $\Sigma_{02}(R) = \frac{\overline{\Sigma_d(R=0)}\frac{(1-R)}{(1-\kappa R)}}{\Gamma(1+{}^1/_{m_2}){J_{m2}}^{-1/m_2}}$ and Γ is the Euler function, defined as $\Gamma(t) = \int_0^\infty x^{t-1}e^{-x}dx$.

$\overline{\Sigma_d}$ is the average experimentally determined fatigue limit. The spatial integration allows all potential propagation sites to be taken into account as well as to better account for multiaxial loading conditions.

6.3 The total probability of survival

The total probability of survival on the component is defined by again applying the hypothesis of the weakest link. It is obtained by multiplying the two survival probabilities from the two different observed mechanisms:

$$1 - P_F = (1 - P_{F1})(1 - P_{F2})$$

The entire process can be represented in the form of a probabilistic Kitagawa type diagram, schematically shown in Figure 7, which describes the competition between the two observed mechanisms. Thanks to the probabilistic framework the scatter associated with each mechanism is explicitly taken into account.

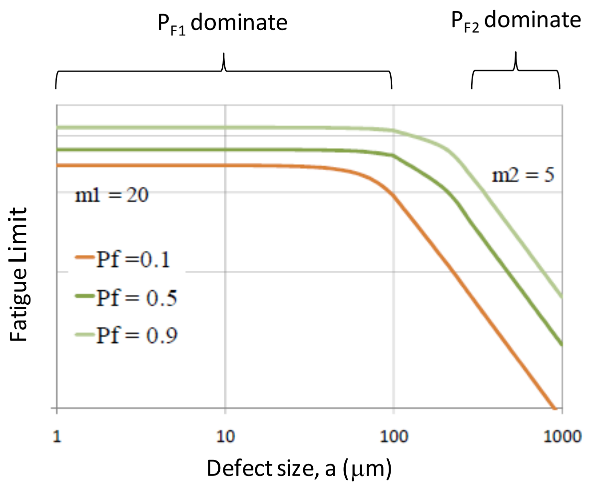

Figure 7. Schematic probabilistic Kitagawa type diagram

6.4 Critical analysis of the proposed model

In order to compare the predictions of the proposed model with the experimental data presented above for different loading conditions (i.e. plane bending, axisymmetrical bending and torsion), the [Dang Van 1973] representation is chosen (see Figure 8). The dotted line on the diagram corresponds to the Dang Van criterion, identified by the torsional and plane bending experimental fatigue limits, for an R-ratio of R=-1. It can be seen that the predictions of the proposed criterion (i.e. the non-solid data points) are in general less conservative and closer to the experimental data (i.e. the solid data points) than the Dang Van criterion. Figure 8 highlights the fact that the Dang Van criterion has difficulty prediction the fatigue behavior of this type of material.

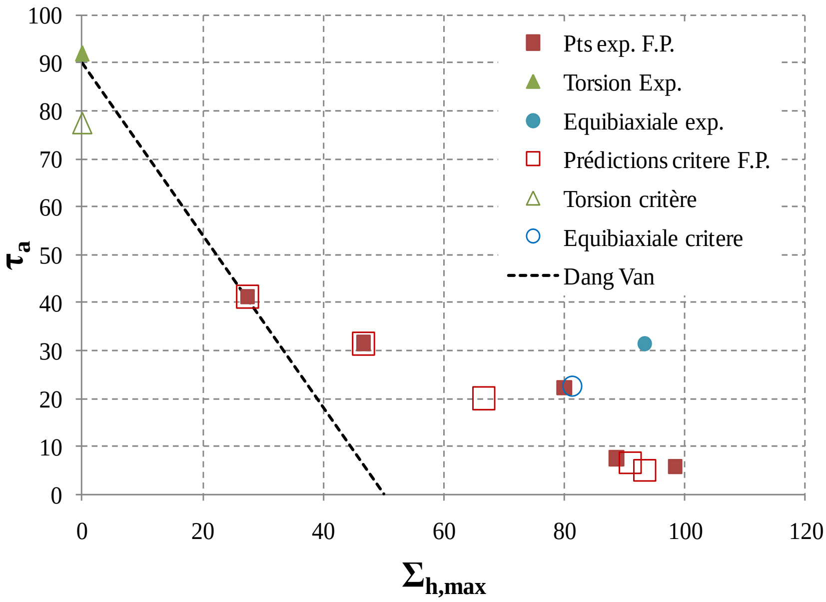

Figure 8. Dang Van diagram, showing the predictions of the proposed criterion and the corresponding experimental data for the cast aluminium alloy AlSi7Cu05Mg03-T7

7 CONCLUSIONS AND PROSPECTS

The principal objective of this work was to develop a probabilistic high cycle fatigue model adapted to Al-Si cast aluminum alloys, which is able to take into account the different microstructural heterogeneities present in the material and has the capacity to reproduce the experimentally observed tendencies for very different multiaxial loading conditions.

Based on a large number of data taken from the literature and the vast experimental campaign undertaken by the authors, it has been concluded that two coexisting fatigue damage mechanisms occur in this material. When the influence of micro-shrinkage pores is reduced, by a HIP treatment for example, the multiaxial fatigue behavior is controlled via meso-plasticity occurring in the material matrix. This is very different from that observed with a typical gravity cast material, for which the dominate fatigue crack leading to final fatigue typically occurs at a micro-shrinkage pore. It is important to note that, even in this case, the first damage mechanism is still present, but rarely leads to failure.

In order to take into account both of these damage mechanisms, a probabilistic approach using a weakest link concept is used to model the “competition” between the two mechanisms. This approach leads naturally to a probabilistic type Kitagawa type diagram, which in this case explains the relationship between the fatigue behaviour of the material and the different casting processes (i.e. gravity casting and HIP).

It is shown that the proposed model is capable of reproducing the experimentally observed tendencies, with respect to both the mean stress effect and the loading mode (torsion, uniaxial tension and equibiaxial tension)

8 ACKNOWLEDGMENTS

This work was undertaken in partnership with PSA Peugeot Citrooën and was financially supported by the French region, Pays de la Loire.

9 REFERENCES

Bellett D., Morel F. and Nguyen M., (2005), Influence des fortes contraintes hydrostatiques sur la résistance en fatigue d’un alliage d’aluminium AS7G03U, Rapport technique final, centre Angers.

Comte F., Maclan N., Morin N., Maitournam H. and Moumni Z., (2005), Prise en compte des contrainte résiduelles de traitement thermique dans la prédiction de la tenue en service des culasses en aluminium, Proceedings of 17eme Congrès Français de Mécanique, Troyes, France Vol. 6 No 3, pp.343-348

Dang Van K., (1973), Sur la résistance à la fatigue des Métaux, Sciences et techniques de l'armement.

Duparque C., Augustins L., Morel F. and Bellett D., (2011), Machine d'essai en fatigue biaxiale disposant d'une éprouvette, French Patent, submitted 17 May 2011, n° de demande 1154287, n° de soumission 1000112324

Huyen Nguyen Thi Thu, (2008), Effet des hétérogéneités microstructurales sur le comportement en fatigue multiaxiale à grand nombre de cycles. PhD thesis. Arts et Métiers ParisTech Centre d’Angers LPMI.

Koutiri I., (2011), Effet des fortes contraintes hydrostatiques sur la tenue en fatigue des matériaux métalliques, PhD thesis. Arts et Métiers ParisTech Centre d’Angers LAMPA.

Murali S., Arvind T.S., Raman K.S. and Smurthy K.S., (1997), Mater.Trans. JIM 38, 28.

Pessard E., Morel F., Morel A. and Bellett D., (2011), Modelling the role of non-metallic inclusions on the anisotropic fatigue behaviour of forged steel, International Journal of Fatigue, Vol. 33, pp. 568–577

Powell G.W., (1994), Mater. Charact. 33, 275.

Skallerud B., Iveland T., and Harkegard G., (1993), Fatigue life assessment of aluminum alloys with casting defects Engineering Fracture Mechanics Vol.44, No.6, pp. 857-874.